Pose Recognition in Indoor Environments using a Fisheye Camera and a Parametric Human Model

K. K. Delibasis [1], V. P. Plagianakos [1] and I. Maglogiannis [2]
[1]*University of Central Greece, Department of Computer Science and Biomedical Informatics, Lamia, Greece*
[2]*University of Piraeus, Dept. of Digital Systems, Piraeus, Greece*

Keywords: Human Activity Detection, Computer Vision, Fisheye Camera Modeling, 3D Human Modeling, Posture Recognition.

Abstract: In this paper we present a system that uses computer vision techniques and a deformable 3D human model, in order to recognize the posture of a monitored person, given the segmented human silhouette from the background. The video data are acquired indoors from a fixed fish-eye camera placed in the living environment. The implemented 3D human model collaborates with a fish-eye camera model, allowing the calculation of the real human position in the 3D-space and consequently recognizing the posture of the monitored person. The paper discusses the details of the human model and fish-eye camera model, as well as the posture recognition methodology. Initial results are also presented for a small number of video sequences, of walking or standing humans.

1 INTRODUCTION AND RELATED WORK

The field of automated human activity recognition utilizing fixed cameras in indoor environments has gained significant interest during the last years. It finds a wide variety of applications in diverse areas, such as assistive environments, supporting the elderly or the chronic ill, surveillance and security, traffic control, industrial processes etc. This work focuses in pose estimation of walking or standing human from fisheye video: therefore human silhouette segmentation of the video sequence is a prerequisite. The proposed algorithm is based on a parametric three-dimensional (3D) human model that can move its legs and arms, as well as on a model of the fisheye camera that allows the rendering of the parametric model. An evolutionary optimization algorithm is used to recover the parameters of the 3D human model.

The first step in applications dealing with human activity recognition from video is foreground segmentation. Most of the video segmentation algorithms are based on background subtraction. The background has to be modelled, since it may change due to a number of reasons, including: motion of background objects, differences in light conditions, or video compression artefacts. Therefore, a number of techniques have been proposed for constructing a model of the background that is being gradually updated using the values of the current video frame. In (Willems 2009) the background model is defined as the previous frame. Background can be modelled by median filtering (Cucchiara 2003) of a predefined number of last frames that are hold in a buffer. The background value of each pixel in the model is independently computed as the temporal median of the pixel values along the buffer. This approach however may become slow for large frame sizes. Other approaches (eg. McFarlane and Schofield 1995, or the running average Willems 2009) use an incremental update of the background, without the need of a buffer to store previous frames. An extension of the aforementioned methods is the running Gaussian average which was proposed in (Wren 1997). A more complex but popular segmentation algorithm is the Mixture of Gaussians (MoG), initially described for video sequences by Stauffer and Grimson (1999).

In this work we have performed video segmentation using the illumination sensitive method (Cheng 2011), as implemented in (Christodoulidis 2012). This technique is based on the entropy calculation of each frame and it solves the problem of sudden illumination changes, which

Delibasis K., Plagianakos V. and Maglogiannis I..
Pose Recognition in Indoor Environments using a Fisheye Camera and a Parametric Human Model.
DOI: 10.5220/0004693704700477
In *Proceedings of the 9th International Conference on Computer Vision Theory and Applications* (VISAPP-2014), pages 470-477
ISBN: 978-989-758-004-8

affect significantly the background modelling. Therefore it is considered appropriate for the proposed system.

Regarding the human silhouette modelling, articulated stick human models are quite popular for pose estimation. Volumetric human models use geometric primitives such as are spheres, cylinders or tapered super-quadrics (Delamarre 2001), (Kehl 2006). Surface-based models of the human body typically consist of a mesh of polygons that may be deformed (Barron 2001).

Pose estimation is achieved by recovering the values of the human model parameters. A number of reported works use the "top-down estimation", by comparing the rendered 3D human model with the actual frame, using local search methods (Bregler 2004).

A small number of approaches use information about the camera model and setting, to assist pose recovery. In (Taylor 2000) the perspective information of a mono-occular camera is used. In (Liebowitz 2003) reconstruction of 3D poses from 2D point correspondences is reported, using multiple views and known body segment lengths. Detailed description of these approaches can be found in the survey of (Poppe 2007).

In the proposed system video is captured using 360 degrees field of view (FoV) hemispheric cameras, also known as fisheye cameras. The utilization of fisheye cameras is increasing both in robotic applications and in video surveillance (Kemmotsu 2006), (Zhou 2008). In (Saito 2010) a probabilistic model of pedestrians imaged by a fisheye camera is utilized. As fisheye cameras with megapixel sensors are now available, research in calibration of such cameras becomes increasingly useful. Thus, the topic of fish-eye camera calibration has attracted significant attention, on its own. In (Li 2006) and (Basu 1993) the calibration of fisheye camera is reported using high degree polynomials to emulate the strong deformation effects introduced by the fisheye lens. In (Shah 1996) a detailed model is presented for fisheye camera calibration, which estimates the radial and tangential deformation, using a polynomial mapping between the radial distance from the optical axis of a real world point and its imaged point on the image plane. In this work, we employ the forward and inverse camera model that was proposed in (Delibasis 2013).

Regarding human modeling we employ a simple triangulated 3D parametric model with a number of degrees of freedom and follow a "top-down" approach by matching the model rendered through the calibrated fisheye camera, with the segmented frame of the video. Evolutionary optimization is used to recover the model parameters and determine human motion and pose. The range of the parameters of the model is narrowed, using the segmentation refinement algorithm that we proposed in (Delibasis 2013). The rest of the paper is structured as follows: Section 2 discuss the technical details of the proposed algorithms and techniques, Section 3 presents some initial results and finally Section 4 concludes the paper.

2 MATERIALS AND METHODS

2.1 Overall Architecture

The overall architecture of the proposed system is illustrated in Fig. 1. It comprises of a) a model of the fisheye camera that enables the extraction of the direction of view of each pixel of the video frame (originally proposed in Delibasis 2013), b) a 3D parametric model of a human and c) an evolutionary algorithm that recovers the parameters of the 3D human model, based on an objective function that compares the rendering of the 3D model through the camera model to the segmented human.

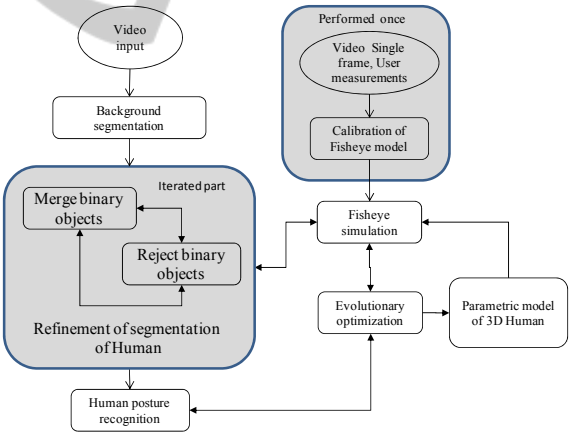

Figure 1: The overall system architecture.

2.2 Fisheye Camera Model

The main characteristic of the fisheye camera is that it can cover a field of view of 180 degrees. We use a model to simulate the image formation using the fisheye camera, so that given the real-world position of an object (x,y,z), we may calculate the image coordinates (j,i) of its pixels. The action of the fisheye model M can be written in the general form

$$(j,i) = M(x,y,z) \quad (1)$$

We adopted a model for the fisheye camera that is based on the physics of image formation, as described in (Max 1983), (Greene 1986) and demonstrated in (http://paulbourke.net/ dome/ fisheye/) and (Delibasis 2013). We consider a spherical element of arbitrary radius R_0 with its center at $K(0,0,z_{sph})$ (as it will become clear soon, the radius R_0 is not a parameter of the model). For any point P with real world coordinates (x,y,z), we determine the intersection Q of the line KP with the spherical optical element of the fisheye lens. The point P is imaged at the central projection (x_{im}, y_{im}) of Q on the image plane with equation $z=z_{plane}$, using the $O(0,0,0)$ as center of projection, assuming that the installation of the camera is such that the imaging plane (i.e. the image sensor) is horizontal and the axis of the spherical lens is not misaligned. Thus, it becomes obvious that all real world points that lie on the KP line are imaged at the same point (x_{im}, y_{im}) of the image plane. The KP line is uniquely defined by its azimuth and elevation angles, θ, φ respectively. The concept of the fisheye geometric model is shown in Fig. 2.

The fisheye camera has no moving parts. Therefore, the ratio $p = z_{sph}/z_{plane}$ is the primary parameter of the fisheye model. z_{plane} is set to an arbitrary value less than R_0, thus $z_{sph} = pz_{plane}$. It is possible that small internal lens misalignments may introduce unanticipated imaging deformations (Shah 1996). Thus, we introduce two extra model parameters, the X and Y position of the center of spherical lens x_{sph}, y_{sph} with respect to the optical axis of the camera. Now the center of the spherical element becomes $K(x_{sph}, y_{sph}, z_{sph})$. Fig. 2 shows the case for $x_{sph} = 0, y_{sph} = 0$ for simplicity. The position of any point of the line segment KP, thus Q as well, is given by

$$(Q_x, Q_y, Q_z) = \lambda (x - x_{sph}, y - y_{sph}, z - z_{sph}) \quad (2)$$

where λ is a parameter in range [0,1].

If we insert this into the equation of the spherical optical element, we derive an equation whose solution defines λ and the position of Q:

$$\begin{aligned} &\left(\lambda(x - x_{sph}) - x_{sph}\right)^2 + \left(\lambda(y - y_{sph}) - y_{sph}\right)^2 \\ &+ \left(\lambda(z - z_{sph}) - z_{sph}\right)^2 - R_0^2 = 0 \end{aligned} \quad (3)$$

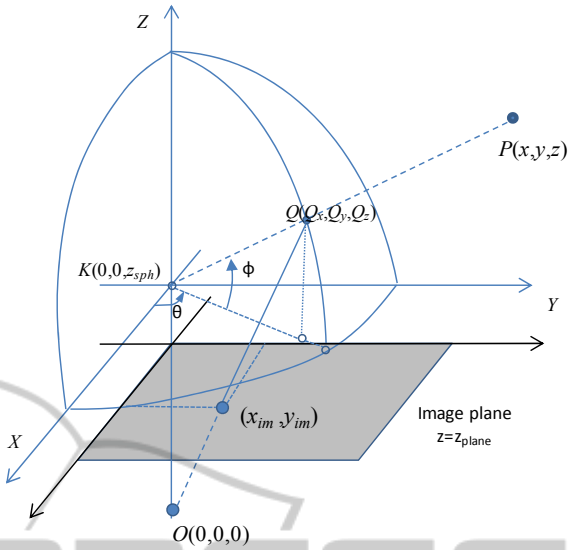

Figure 2: The geometry of the fisheye model.

The final step is the calculation of the central projection (x_{im}, y_{im}) of Q on the image plane:

$$(x_{im}, y_{im}) = \frac{z_{plane}}{z_{sph}} (Q_x, Q_y) \quad (4)$$

For any point P with real world coordinate $z>z_{sph}$, its projection onto the image plane (x_{im}, y_{im}) is bounded by the radius of the virtual spherical optical element R_0: $-R_0 \le x_{im} - x_{sph} \le R_0$. When $x \to \infty$ then $(x_{im} - x_{sph}) \to R_0$. The same holds for the y coordinate. The image pixel (i,j) that corresponds to (x_{im}, y_{im}) is calculated by a simple linear transform:

$$(j,i) = (x_{im}, y_{im}) \frac{R_{FoV}}{R_0} + (CoD_x, CoD_y) \quad (5)$$

where (CoD_x, CoD_y) is the center of distortion pixel that corresponds to elevation $\varphi=\pi/2$ and R_{FoV} is the radius of the circular field of view (FoV). For the fish-eye camera, (Micusik 2006) suggests that the CoD is located as the center of the circular field-of-view (see Fig. 3 for a typical video frame). We therefore apply the canny edge detector, using a standard deviation equal to 2 in order to detect the stronger edges in the image, which are the edges of the circular field of view. Then, we employ a simple least squares optimization to obtain the CoD and the radius of the FoV. This is done only once, during the calibration of the camera model.

The calibration process of the camera model recovers the values of the unknown p, x_{sph}, y_{sph}

parameters. The user provided the position of N_p=18 landmark points $\left\{\left(X_{im}^i, Y_{im}^i\right)\right\}, i = 1,2,...,N_p$ on one video frame. The real world coordinates of these landmark points $\left\{\left(x_{real}^i, y_{real}^i, z_{real}^i\right)\right\}$ were also measured. The expected position of the landmark points on the video frame, according to the model parameters are (superscripts are not powers):

$$\left(x_{im}^i, y_{im}^i\right) = M\left(x_{real}^i, y_{real}^i, z_{real}^i; p, x_{sph}, y_{sph}\right) \quad (6)$$

The values of the model parameters are obtained by minimizing the error between the expected and the observed frame coordinates of the landmark points:

$$\left(p, x_{sph}, y_{sph}\right) = \arg\min_{p, x_{sph}, y_{sph}} \left(\sum_{i=1}^{N_p} \left(\left(X_{im}^i - x_{im}^i\right)^2 + \left(Y_{im}^i - y_{im}^i\right)^2 \right) \right) \quad (7)$$

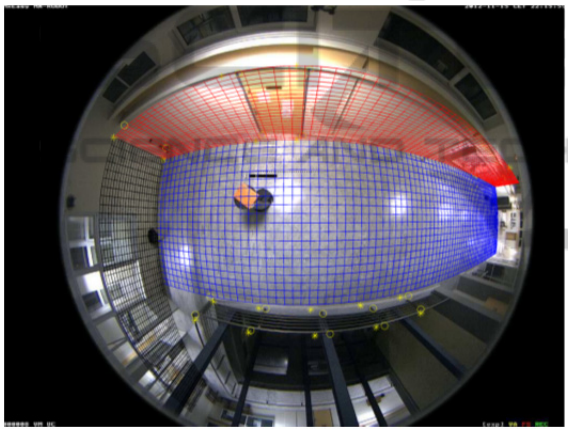

Figure 3: Visualization of the resulting fisheye model calibration.

This minimization is performed by exhaustive search in just few minutes using the Matlab programming environment in an average personal computer. Since the fisheye camera was permanently installed on the roof of the university laboratory, the calibration of the model is performed only once. The resulting calibration of the fisheye model is shown in Fig. 4, where a virtual grid, laid on the floor and on the two walls of the imaged room, is rendered on the captured frame, using the fisheye model. The user-defined landmark points are shown as 'o', whereas their projected location on the video frame, using the calibrated model are shown as '*'.

2.3 Human Model

In this work, we utilized a free triangulated model of a standing human, of 27.000 vertices (http://www.3dmodelfree.com/models/20966-0.htm), approximately. Since we are interested in simulating the rendering of the human model through the fisheye camera in real time, we discard the triangle information of the model and we treat it as a cloud of points. We also applied a vertex decimation process to reduce the number of vertices by a factor of 8.

The vertices of the model were labelled using logical spatial relations, into 5 classes: right and left arm, right and left leg and the rest of the body (torso and head). The pose of the human is modified by changing the position of the hands and legs independently, using the following controlling parameters. Legs are allowed to rotate round the *Y* axis with respect to the hips (thus they remain on the sagital - *YZ* plane). Arms are allowed to rotate round the shoulders. Fig. 4 shows an example of the parametric human model along the coronal and the sagital plane.

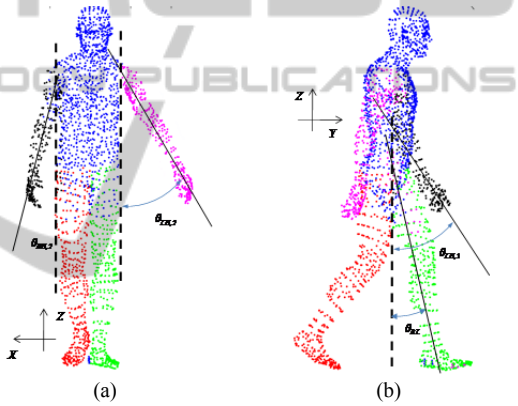

(a) (b)

Figure 4: The model of the human (anterior view and right view), with labels as color. The axis of the limbs and their angles with the vertical human axis, that define the parameters of the 3D human model, are also shown.

The rotation of the hands involves all three Euler angles. In order to avoid dependence on the order of rotation and possible gimbal lock, we utilized the following matrix, that transforms, a unit vector **v**=(*a*,*b*,*c*) on the *Z* axis.

$$\mathbf{A} = \begin{pmatrix} \frac{\lambda}{|v|} & \frac{-ab}{\lambda|v|} & \frac{-ac}{\lambda|v|} & 0 \\ 0 & \frac{\lambda}{c} & \frac{-b}{c} & 0 \\ \frac{a}{|v|} & \frac{b}{|v|} & \frac{c}{|v|} & 0 \\ 0 & 0 & 0 & 1 \end{pmatrix}, \lambda = \sqrt{b^2 + c^2} \quad (8)$$

Assuming that **v** coincides with the axis of the hand, matrix **A** is applied to the vertices of the two hands separately, using homogeneous coordinates.

In addition to the 6 parameters that control the arms and legs of the model, global parameters are also introduced that control: the model's location (x and y translation), size (x, y and z scaling) and global rotation round the Z axis. In order to narrow the range of these global parameters, we utilized the geometric reasoning-based segmentation refinement that we reported in (Delibasis 2013, section 2.4). More specifically we utilize the calibrated fisheye camera model to obtain an estimation of the real (x_{real}, y_{real}) positions of the segmented human. Some instances of the segmented human from a typical video are shown in Fig. 5(a), whereas the path of the walking human in the real world frame of reference is plotted in Fig. 5(b), as estimated using the segmentation refinement (Delibasis 2013, section 2.4). The path is overlaid back on the composite video frame (Fig. 5a) using the forward fisheye model (Delibasis 2013, section 2.2).

The estimated (x_{real}, y_{real}) coordinates are used to initialize the model's location (x and y translation). The global rotation round the Z axis, is calculated using the direction θ_z of the velocity vector (assuming that the human is facing towards the direction that he/she is walking), as following:

$$\theta_z = \tan^{-1}\left(\frac{\bar{y}_t - \bar{y}_{t-1}}{\bar{x}_t - \bar{x}_{t-1}}\right) \quad (9)$$

where $\bar{x}_t = \frac{1}{3}\left(x_{real}^{t} + x_{real}^{t-1} + x_{real}^{t-2}\right)$ is the running average of the last estimated real world coordinates (same hold for y_{real} coordinate), which prevents amplification of the noise, induced by errors in position estimation.

If the human is stationary ($|\bar{x}_t - \bar{x}_{t-1}| < d_0$ AND $|\bar{y}_t - \bar{y}_{t-1}| < d_0$, d_0=0.1) then the angle θ_z is not utilized for narrowing the range of z-rotation angle, which is then set to [0,2π]. The range of the model parameters are shown in Table 1.

The human model is used to produce a simulated (rendered) segmented video frame that is compared to the actually segmented one. A model of a standing man is shown in Figure 6(a), scaled to height=1.8 m and it is placed at several locations in the imaged room, touching the floor. The rendered frame using the fisheye model is shown in Fig.6(b).

The human pose can be extracted by recovering the values of the parameters of the human model in vector $\mathbf{p_m}$. Let us denote by I_M the binary image of the parametric model generated by the fisheye model and by I_S the segmented image of the corresponding video frame.

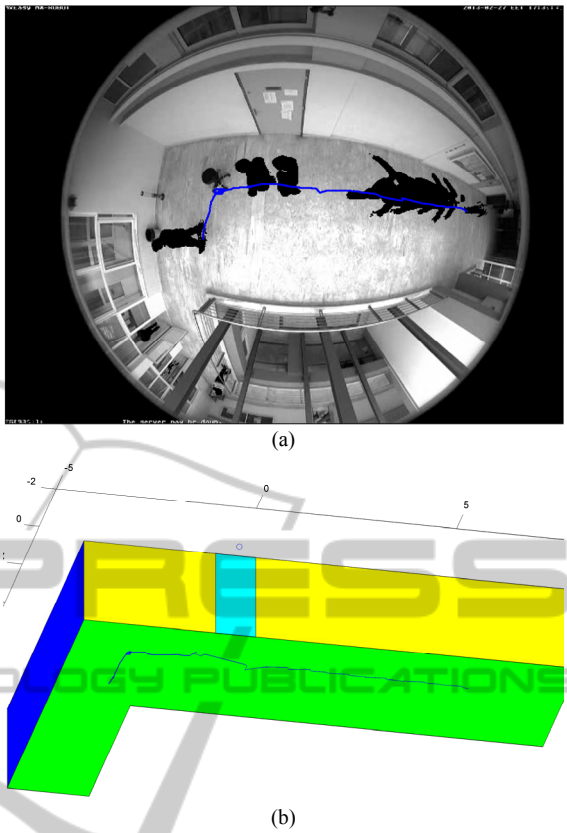

(a) (b)

Figure 5: The resulting segmentation for a number of frames (a) and the estimated path of the walking person in real world coordinates, using the geometric reasoning-based refinement of segmentation proposed in (Delibasis 2013) (b).

Table 1: The parameters of the 3D human model.

Parameter	Min. value	Max. value
X translation	x_{real} -0.4	x_{real} +0.4
Y translation	y_{real} -0.4	y_{real}+0.4
Scaling (independently in 3 axis)	0.8	1.2
Z-rotation	θ_z -π/8	θ_z +π/8
Right, Left Leg angle	-π/6	π/6
Right arm coordinate *a*	-0.9	0
Right arm coordinate *b*	-0.4	+0.4
Right arm coordinate *c*	-1	0
Left arm coordinate *a*	0	0.9
Left arm coordinate *b*	-0.4	+0.4
Left arm coordinate *c*	0	+1

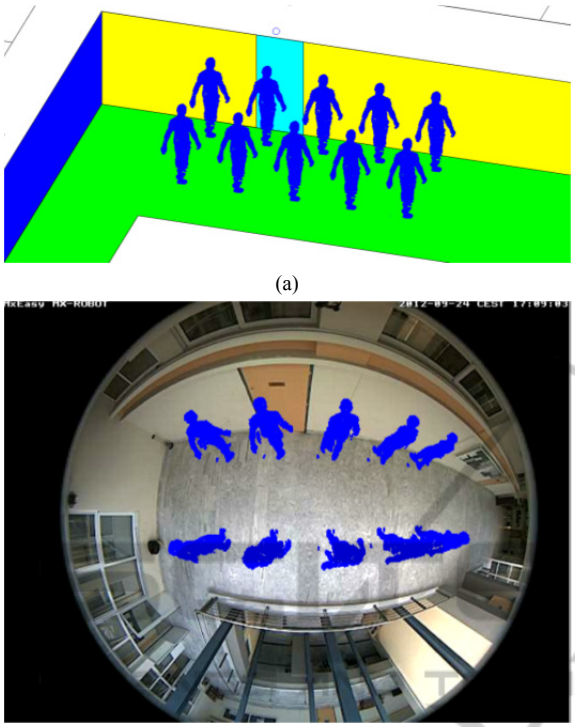

(a) (b)

Figure 6: (a) scaling the model to height=1.8 m, touching the floor and reproducing the model at several locations of the imaged room and (b) rendering the 3D human models through the calibrated fisheye lens.

The objective function is defined as following:

$$f(\mathbf{p_m}) = \sum_{\substack{image \\ domain}} I_M \cap I_S - \sum \bar{I}_M \cap I_S - \sum I_M \cap \bar{I}_S \quad (10)$$

where, $\bar{I}$ denotes the boolean negative of I, $\cap$ denotes the boolean AND operator and the summation is done over the whole image domain. The objective function is defined as the number of non-zero pixels of I_M on non-zero pixels of I_S minus the number of non-zero pixels of I_M on zero pixels of I_S, minus the number of zero pixels of I_M on non-zero pixels of I_S. Thus, the objective function should be maximized.

Due to the large number of parameters and the complexity of the objective function, which cannot be written in closed form and its derivatives cannot be analytically computed, we employed a simple Genetic Algorithm as an optimizer. The simple GA is a generational one, as described in (Goldberg 1999), it uses real encoding, one-point crossover, a population of 80 chromosomes and it is allowed to converge for a maximum number of 1000 function evaluations. The probability of crossover and mutation was set to 0.8 and 0.01 respectively. For these initial results, the step of evolutionary optimization is not performed in real time. In the Discussion section, we provide details about execution times as well as future work towards the direction of near real time execution.

3 EXPERIMENTAL RESULTS

The video sequences used in this work were acquired using the Mobotix Q24 hemispheric camera, which was installed on the ceiling of the imaged room. The pixilation of each frame is 480x640.

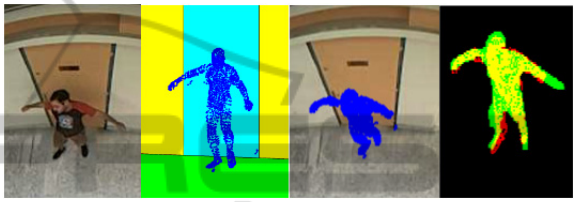

(a) (b) (c) (d)

Figure 7: (a) An original video frame showing a human, (b) the 3D model with its parameters fitted to the segmented original frame, (c) the fisheye-rendered 3D model in a simulated frame and (d) the matching (yellow) between the segmented human (green) and the fisheye-rendered model (red).

Figure 7 shows results from a typical frame (a). The recovered 3D human model is shown in (b) and the rendered 3D human model using the fisheye model is shown in (c). The fitting of the fisheye-rendered parametric 3D human model to the segmented frame is shown in Fig. 7(d), as following: segmented frame in green, the fisheye rendered 3D human in red and their intersection in yellow. It can be observed that the proposed algorithm was able to detect the specific human pose. Initial results were obtained by testing the proposed algorithm in 5 video sequences of 1500 – 2000 frames, of a walking or standing human. In Fig. 8a, the resulting segmentation from a number of frames is shown in a single composite frame. The results of fitting the fisheye-rendered 3D human model to the actual segmented human silhouette using GAs-based optimization is shown in (8b) (same colours as in Fig.(7)). In (8c) the recovered 3D human models are shown in the real world space. These experiments show that it is feasible to extract the human pose from a significant percentage the fisheye video frames, even imperfect segmentation.

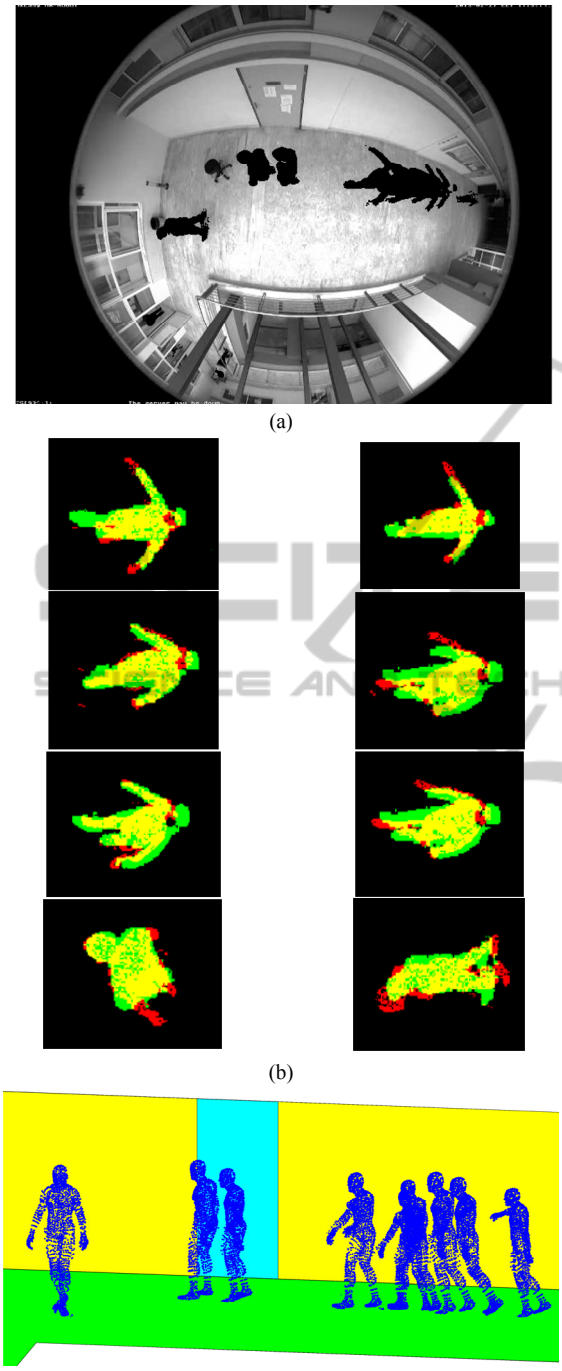

(a)

(b)

(c)

Figure 8: (a) a single composite frame the resulting segmentation from a number of frames. (b) The fisheye-rendered parametric 3D human models fitted to the segmented frames (see text). (c) the recovered 3D human models in the Cartesian space.

4 CONCLUSIONS

A methodology for human pose recognition has been presented in this paper. The proposed algorithms are based on a deformable 3D human model, a parametric model of the specific fisheye camera and a top-down approach using GAs-based optimization. Given the video foreground segmentation refinement and its geometry-based refinement, the algorithm estimates the human's position and pose, considering the orientation of its limbs. Initial results have been presented that show the feasibility of the proposed methodology.

The generation of the 3D parametric human model is performed in approximately 1 msec. The rendering of a 3D human model with 2.500 vertices through the modelled fisheye camera is also performed in 1.5 msec. The calculation of the objective function (Eq. 10) requires approx. 8 msec for a 3D model with 2.500 vertices and a frame of 480x640 pixels. All timing was performed using an Intel(R) Core i5-2430 CPU @ 2.40 GHz Laptop with 4 GB Ram, under Windows 7 Home Premium. The code was developed using the Matlab programming environment. No special code optimization or any kind of parallelization was performed. It becomes clear that the optimization of the objective function in order to extract the human pose has not been performed in real time. At this stage, these initial results serve as proof of concept that the proposed algorithm is feasible. Further work will include, the adoption of a more robust statistical 3D model for the human and the refinement of the fisheye model, using more parameters to increase its accuracy. Finally more efficient implementation of the genetic algorithm based optimization will be explored for the determination of the 3D model parameters. These approaches include exploiting the converged population from the previous frames to initialize the search for the current frame and/or restricting the parameter range according to their optimal values from the previous frames.

ACKNOWLEDGEMENTS

The authors would like to thank the European Union (European Social Fund ESF) and Greek national funds through the Operational Program "Education and Lifelong Learning" of the National Strategic Reference Framework (NSRF) - Research Funding Program: \Thalis \ Interdisciplinary Research in Affective Computing for Biological Activity

Recognition in Assistive Environments for financially supporting this work.

REFERENCES

Willems J., Debard G., Bonroy B., Vanrumste B. and Goedemé T., "How to detect human fall in video? An overview", In *Proceedings of the positioning and contex-awareness international conference* (Antwerp, Belgium, 28 May, 2009), POCA '09.

Cucchiara, R., Grana, C., Piccardi, M., and Prati A. 2003. Detecting moving objects, ghosts, and shadows in video streams. *IEEE Transactions on Pattern Analysis and Machine Intelligence* 25, 10, (2003), 1337-1442.

McFarlane, N. and Schofield C., "Segmentation and tracking of piglets in images", *MACH VISION APPL.* 8, 3, (May. 1995), 187-193.

Wren, C., Azarhayejani, A., Darrell, T., and Pentland, A. P. 1997. Pfinder: real-time tracking of the human body, *IEEE Transactions on Pattern Analysis and Machine Intelligence* 19, 7, (October. 1997), 780-785.

Stauffer C., and Grimson W., "Adaptive background mixture models for real-time tracking". In *Proceedings of the conference on computer vision and pattern recognition* (Ft. Collins, USA, June 23-25, 1999), CVPR '99. IEEE Computer Society, New York, NY, pp. 246-252.

Cheng F. C., Huang S. C. and Ruan S. J. 2011, Implementation of Illumination-Sensitive Background Modeling Approach for Accurate Moving Object Detection, *IEEE Trans. on Boardcasting*, vol. 57, no. 4, pp.794-801, 2011.

Christodoulidis A., Delibasis K., Maglogiannis I., "Near real-time human silhouette and movement detection in indoor environments using fixed cameras", in *The 5th ACM International Conference on PErvasive Technologies Related to Assistive Environments*, Heraklion, Crete, Greece, 2012.

Delamarre, Q., Faugeras, O., "3D articulated models andmultiview tracking with physical forces", *Computer Vision and ImageUnderstanding* (CVIU) 81 (3) (2001) 328–357.

Kehl, R., Van Gool, L., "Markerless tracking of complex human motions from multiple views", *Computer Vision and Image Understanding* (CVIU) 104 (2–3) (2006) 190–209.

Barron, C., Kakadiaris, I., "Estimating anthropometryand pose from a single uncalibrated image", *Computer Vision andImage Understanding* (CVIU) 81 (3) (2001) 269–284.

Bregler, C., Malik, J., Pullen, K., "Twist basedacquisition and tracking of animal and human kinematics", *International Journal of Computer Vision* 56 (3) (2004) 179–194.

Taylor, C., Reconstruction of articulated objects from point correspondences in a single uncalibrated image, *Computer Vision and Image Understanding* (CVIU) 80 (3) (2000) 349–363.

Liebowitz, D., Carlsson, S., "Uncalibrated motion captureexploiting articulated structure constraints", *International Journal of Computer Vision* 51 (3) (2003) 171–187.

Poppe, R., "Vision-based human motion analysis: An overview", *Computer Vision and Image Understanding*, 108 (2007) 4–18.

Kemmotsu, K., Tomonaka, T., Shiotani, S., Koketsu, Y., and Iehara, M., "Recognizing human behaviors with vision sensors in a Network Robot System," *IEEE Int. Conf on Robotics and Automation*, pp.l274-1279, 2006.

Zhou, Z., Chen, X., Chung, Y., He, Z., Han, T. X. and Keller, J., "Activity Analysis, Summarization and Visualization for Indoor Human Activity Monitoring," *IEEE Trans. on Circuit and systems for Video Technology*, Vol. 18, No. II, pp. 1489-1498,2008.

M. Saito and K. Kitaguchi, G. Kimura and M. Hashimoto,"Human Detection from Fish-eye Image by Bayesian Combination of Probabilistic Appearance Models", *IEEE International Conference on Systems Man and Cybernetics (SMC)*, 2010, pp243-248.

Li H. and Hartley R., "Plane-Based Calibration and Auto-calibration of a Fish-Eye" Camera, P.J. Narayanan et al. (Eds.): ACCV 2006, LNCS 3851, pp. 21–30, 2006, c Springer-Verlag Berlin Heidelberg 2006.

Basu A., Licardie S., "Modeling fish-eye lenses", Proceedings of the 1993 *IEEWSJ International Conference on Intelligent Robots and Systems* Yokohama, Japan July 2630,1993.

Shah S. and Aggarwal J., "Intrinsic parameter calibration procedure for a high distortion fish-eye lens camera with distortion model and accuracy estimation", Pattern Recognition 29(11), 1775- 1788, 1996.

Delibasis K. K., Goudas T., Plagianakos V. P. and Maglogiannis I., Fisheye Camera Modeling for Human Segmentation Refinement in Indoor Videos, in *The 6th ACM International Conference on PErvasive Technologies Related to Assistive Environments*, PETRA 2013.

Max, N., "Computer Graphics Distortion for IMAX and OMNIMAX Projection", *Proc Nicograph* 83, Dec 1983 pp 137.

Greene, N., "Environment Mapping and Other Applications of World Projections", *IEEE Computer Graphics and Applications*, November 1986, vol. 6(11), pp 21.

http://paulbourke.net/dome/fisheye/

Micusik, B. and Pajdla, T., "Structure from Motion with Wide Circular Field of View Cameras", *IEEE Transactions on Pattern Analysis and Machine Intelligence*, PAMI 28(7), 2006, pp. 1-15.

http://www.3dmodelfree.com/models/20966-0.htm.

Goldberg D., "Genetic Algorithms in Search, Optimization, and Machine Learning", Addison Wesley, 1989.